A negative value of w_c represents a gap rather than overlap between strip edges.

The basis for parallel-plate capacitance is shown in Fig. 10. For both even and odd modes, $C_p = C_1 + C_2$. Since the strip arrangement is symmetrical in this case, the fringe capacitance is calculated for only one strip. Again, the required expressions for fringing capacitance are found by conventional methods.

Acknowledgment

J. Mosko of Naval Ordnance Test Station, China Lake, Calif., has programmed the design equations for electronic computation. He supplied the data from which Fig. 5 was prepared. He can provide a copy of the Fortran program to anyone who wishes to use it.

References

[1] E. M. T. Jones and J. T. Bolljahn, "Coupled-strip-line filters and directional couplers," *IRE Trans. on Microwave Theory and Techniques*, vol. MTT-4, pp. 75–81, April 1956.

[2] J. K. Shimizu and E. M. T. Jones, "Coupled-transmission-line directional couplers," *IRE Trans. on Microwave Theory and Techniques*, vol. MTT-6, pp. 403–410, October 1958.

[3] S. B. Cohn, "Direct-coupled-resonator filters," *Proc. IRE*, vol. 45, pp. 187–196, February 1957.

[4] S. B. Cohn, "Characteristic impedances of broadside-coupled strip transmission lines," *IRE Trans. on Microwave Theory and Techniques*, vol. MTT-8, pp. 633–637, November 1960.

[5] W. J. Getsinger, "A coupled strip-line configuration using printed-circuit construction that allows very close coupling," *IRE Trans. on Microwave Theory and Techniques*, vol. MTT-9, pp. 535–544, November 1961.

[6] S. B. Cohn, "Shielded coupled-strip transmission line," *IRE Trans. on Microwave Theory and Techniques*, vol. MTT-3, pp. 29–38, October 1955.

[7] H. A. Wheeler, "Transmission-line properties of parallel wide strips by a conformal-mapping approximation," *IEEE Trans. on Microwave Theory and Techniques*, vol. MTT-12, pp. 280–289, May 1964.

Theoretical Analysis of Twin-Slab Phase Shifters in Rectangular Waveguide

ERNST SCHLÖMANN

Abstract—**The differential phase shift and the losses to be expected in phase shifters using two oppositely magnetized ferrite slabs located symmetrically in a rectangular waveguide have been calculated for various locations and thicknesses of the ferrite slabs. For small thicknesses of the ferrite slabs, the differential phase shift increases rapidly with increasing thickness reaching a maximum when the thickness is approximately 1/10 of the free space wavelength. The calculated insertion loss of a 360-degree phase shifter decreases with increasing slab thickness for small thickness, reaching a minimum when the thickness is approximately 1/25 of the free space wavelength. The minimum insertion loss calculated with the assumption that the imaginary part of the diagonal component of the permeability tensor is 0.01 and that dielectric loss can be neglected is approximately 0.85 dB. The peak power handling capability has also been analyzed. It can conveniently be summarized in terms of a high-power figure of merit. For reasonably high values of this figure of merit, a peak power capability of the order of 100 kW is anticipated.**

I. Introduction

ONE OF THE more promising device configurations for digital ferrite phase shifters is that of a rectangular waveguide containing circumferentially magnetized ferrite toroids of suitable length [1], [2]. Such a structure is shown in Fig. 1. A very similar structure, which is more readily amenable to theoretical analysis, is shown in Fig. 2. Here the ferrite toroid has been replaced by two oppositely magnetized slabs which extend over the complete height of the waveguide. The propagation of electromagnetic waves through waveguides of the type shown in Fig. 2 has previously been analyzed by Lax et al. [3], [4] and by von Aulock [5]. Here we use substantially the notation of von Aulock.

In the previous work, only the differential phase shift and the field configuration have been discussed. The present paper contains more detailed results than previously published, concerning the differential phase shift and its dependence upon parameters such as spacing, width, dielectric constant, and remanent magnetization of the ferrite slabs. In addition, the present paper contains a discussion of the insertion loss and the peak power limitations of these devices.

For odd TE_{n0}-modes the characteristic equation for the reduced propagation constant Γ can be expressed as

$$\cot \delta = \frac{\nu(1 + \cot \alpha_1 \cot \alpha_2) + \zeta \cot \alpha_1 + \eta \cot \alpha_2}{\cot \alpha_1 \cot \alpha_2 - 1} \quad (1)$$

Manuscript received June 25, 1965; revised September 7, 1965. The work reported in this paper was supported by the U. S. Army Materiel Command under Contract DA 30-069-AMC-333(Y).

The author is with the Raytheon Company, Waltham, Mass.

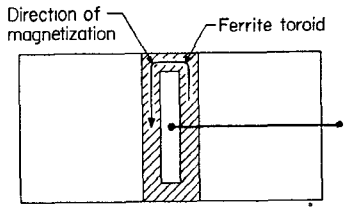

Fig. 1. Phase shifter using ferrite toroid.

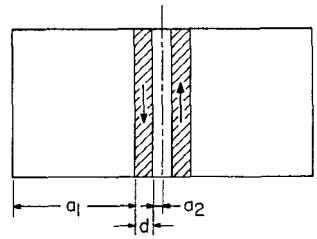

Fig. 2. Phase shifter using twin ferrite slabs.

where

$$\alpha_1 = \frac{2\pi a_1}{\lambda_0}(1 - \Gamma^2)^{1/2}$$

$$\alpha_2 = \frac{2\pi a_2}{\lambda_0}(1 - \Gamma^2)^{1/2}$$

$$\delta = \frac{2\pi d}{\lambda_0}(\epsilon\mu_e - \Gamma^2)^{1/2} \tag{2}$$

$$\nu = \frac{\kappa}{\mu}\frac{\Gamma}{(\epsilon\mu_e - \Gamma^2)^{1/2}}$$

$$\zeta = \mu_e\frac{(1 - \Gamma^2)^{1/2}}{(\epsilon\mu_e - \Gamma^2)^{1/2}}$$

$$\eta = \frac{\epsilon\mu - \Gamma^2}{\mu(1 - \Gamma^2)^{1/2}(\epsilon\mu_e - \Gamma^2)^{1/2}}.$$

The lengths a_1, a_2, and d are explained in Fig. 2. λ_0 is the free space wavelength, ϵ the permittivity, μ the diagonal, $\pm j\kappa$ the off-diagonal component of the permeability tensor, and Γ equals $\lambda_0\beta/2\pi$ where β is the propagation constant. If ϵ, μ, and κ are real, the solution Γ of the characteristic equation (1) is also real. This means that the wave is not attenuated. If ϵ, μ, or κ are complex, however, the solution Γ of this equation is also complex; the imaginary part describing the attenuation of the wave. The effective permeability μ_e in (2) is given by

$$\mu_e = \frac{\mu^2 - \kappa^2}{\mu}. \tag{3}$$

In the present context, the case of near center loading is of particular interest. In this case $\alpha_2 = 0$, and the characteristic equation reduces to

$$\cot\delta = \nu + \eta\tan\alpha_1. \tag{4}$$

Since the characteristic equation (1) is quite involved and depends on a large number of parameters, it is worthwhile to try to simplify it by introducing a reasonable approximation, reducing at the same time the number of significant parameters. The discussion of the characteristic equation which follows shows that in cases of practical interest, the RF fields are strongly concentrated in and near the ferrite slabs, so that the precise location of the side walls of the waveguide becomes immaterial. It is shown, in fact that the differential phase shift is large enough to be of practical interest only when $\Gamma^2 > 1$. This implies that the variation of the electromagnetic field is sinusoidal inside the ferrite, but exponential outside the ferrite. In most cases of practical interest, the exponential decrease of the fields away from the ferrite slabs is so strong that the exact location of the waveguide wall has no substantial influence on the propagation characteristics. This can be derived in a formal way from the characteristic equation (1) by noting that for $\Gamma^2 > 1$, $\cot\alpha_1$ becomes $-j\coth|\alpha_1|$ and, hence, independent of a_1 for $|\alpha_1| \gg 1$. We shall refer to this approximation as the "strong field concentration" approximation.

For convenience, we introduce the abbreviations

$$D = 2\pi d/\lambda_0; \quad A_1 = 2\pi a_1/\lambda_0; \quad A_2 = 2\pi a_2/\lambda_0. \tag{5}$$

The characteristic equation in the strong field concentration approximation $[A_1(\Gamma^2 - 1)^{1/2} \gg 1]$ can then be expressed as

$$\cot D(\epsilon\mu_e - \Gamma^2)^{1/2} = \frac{\frac{\kappa\Gamma}{\mu} + \frac{\epsilon\mu - \Gamma^2}{\mu(\Gamma^2 - 1)^{1/2}} - \left[\frac{\kappa\Gamma}{\mu} + \mu_e(\Gamma^2 - 1)^{1/2}\right]\tanh A_2(\Gamma^2 - 1)^{1/2}}{(\epsilon\mu_e - \Gamma^2)^{1/2}[1 + \tanh A_2(\Gamma^2 - 1)^{1/2}]}. \tag{6}$$

The simplification for the case of center loading ($A_2 = 0$) is obvious. Equation (6) can also be used if $\Gamma^2 > \epsilon\mu_e$. In this case, the left-hand side must be replaced by $\coth D(\Gamma^2 - \epsilon\mu_e)^{1/2}$ and the first factor in the denominator on the right-hand side by $(\Gamma^2 - \epsilon\mu_e)^{1/2}$.

II. Differential Phase Shift

In order to test the validity of the strong field concentration approximation, the characteristic equation (4) (applicable for center loading) has been solved both with and without invoking this approximation. This calculation was carried out for $\epsilon = 11$, $\mu = 1$, and $\kappa = \pm 0.5$. These numerical values are applicable in the case of spinel ferrites at the remanence point if $4\pi M_{\text{rem}}$ equals $\omega/2\gamma$, where ω is the angular frequency and γ the gyromagnetic ratio.

Figure 3 shows the reduced propagation constant Γ as

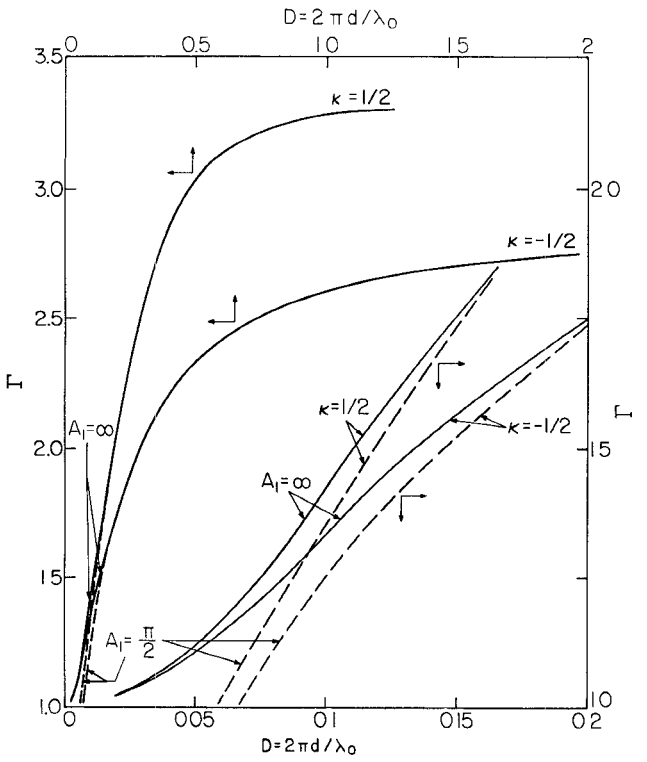

Fig. 3. Reduced propagation constant $\Gamma=\lambda_0\beta/2\pi$ vs. reduced slab width $D=2\pi d/\lambda_0$ for $A_2=0$ (center loading), $A_1=\pi/2$ (empty waveguide at cutoff), and $A_1=\infty$ (strong field concentration approximation). Material constants: $\mu'=1$, $\kappa'=\pm\frac{1}{2}$, $\epsilon'=11$.

a function of reduced slab thickness for center loading. Four separate curves corresponding to $A_1=\pi/2$, $A_1=\infty$, and $\kappa=\pm\frac{1}{2}$ are shown. The lower portion of each curve is replotted on an expanded scale in the lower right-hand corner of the figure. The case $A_1=\infty$ represents the strong field concentration approximation. The case $A_1=\pi/2$ corresponds to a waveguide which is at cutoff in the limit $D\rightarrow 0$. It may be seen that corresponding curves differ appreciably only for small slab thicknesses where the differential phase shift is small and, hence, of little practical interest. This shows that the strong field concentration approximation is reasonably well justified under the conditions encountered in practice.

The characteristic equation applicable in the case of strong field concentration has been solved for arbitrary but relatively small spacing of the slabs. In addition to the previously mentioned numerical example ($\epsilon=11$, $\mu=1$, $\kappa=\pm 0.5$), the calculation was also carried out for $\epsilon=16$, $\mu=1$, $\kappa=\pm 0.25$, ± 0.32, ± 0.4, and ± 0.5. The dielectric constant ($\epsilon=16$) is typical for garnets.

Figures 4–8 show the difference between the reduced propagation constants for the two directions of magnetization (i.e., the differential phase shift per unit length times $\lambda_0/2\pi$) as a function of reduced slab thickness D in the strong field concentration approximation. The four different curves in each figure correspond to A_2 equal to 0, 0.05, 0.1, and 0.2. It may be seen that the differential phase shift increases rapidly with slab thick-

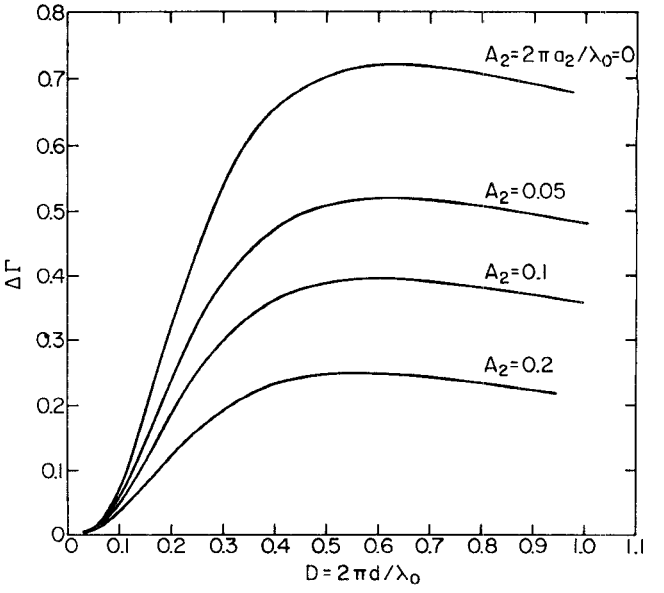

Fig. 4. Reduced differential phase shift $\Delta\Gamma$ vs. reduced slab width D calculated using strong field concentration approximation. Material constants: $\mu'=1$, $\kappa'=\pm 0.5$, $\epsilon'=11$.

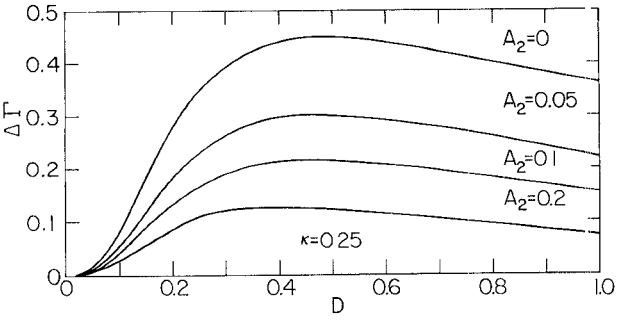

Fig. 5. Reduced differential phase shift $\Delta\Gamma$ vs. reduced slab width D calculated using strong field concentration approximation. Material constants: $\mu'=1$, $\kappa'=\pm 0.25$, $\epsilon'=16$.

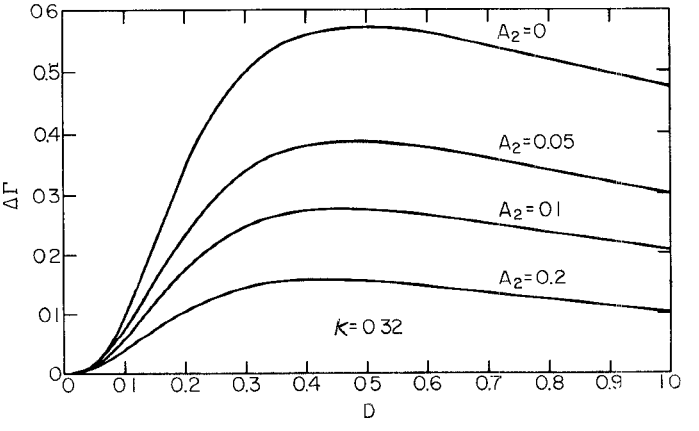

Fig. 6. Reduced differential phase shift $\Delta\Gamma$ vs. reduced slab width D calculated using strong field concentration approximation. Material constants: $\mu'=1$, $\kappa'=\pm 0.32$, $\epsilon'=16$.

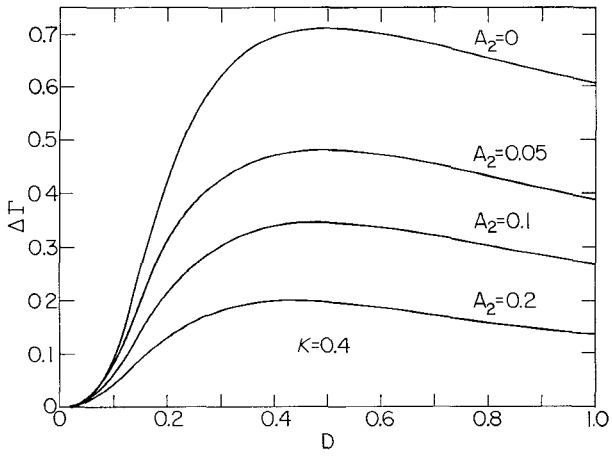

Fig. 7. Reduced differential phase shift $\Delta\Gamma$ vs. reduced slab width D calculated using strong field concentration approximation. Material constants: $\mu'=1$, $\kappa'=\pm 0.44$, $\epsilon'=16$.

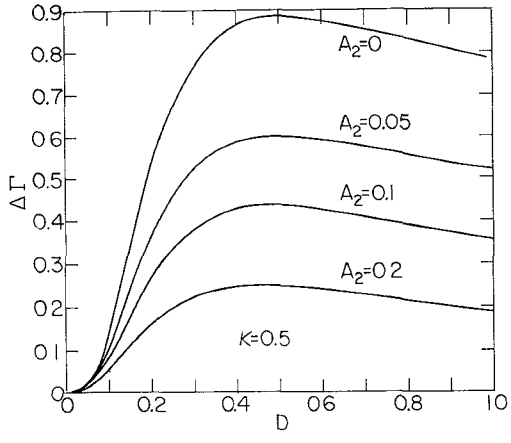

Fig. 8. Reduced differential phase shift $\Delta\Gamma$ vs. reduced slab width D calculated using strong field concentration approximation. Material constants: $\mu'=1$, $\kappa'=\pm 0.5$, $\epsilon'=16$.

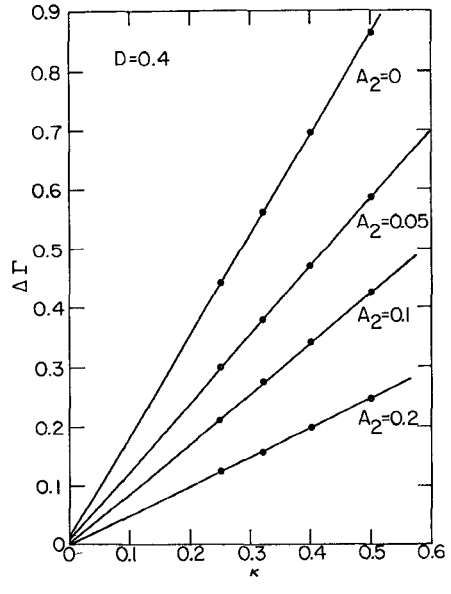

Fig. 9. Reduced differential phase shift $\Delta\Gamma$ vs. κ' (the off-diagonal component of the permeability tensor) for $D=0.4$ and various slab spacings A_2.

ness when the slab thickness is small, and that it reaches a maximum when $D\simeq 0.6$, or $D\simeq 0.5$ for $\epsilon=11$ and $\epsilon=16$, respectively. The differential phase shift also depends fairly sensitively on the slab spacing A_2, being largest for $A_2=0$.

A numerical example is instructive. For S band ($f=3$ Gc/s) a slab thickness of $\frac{1}{4}$ inch and a slab spacing of $\frac{1}{16}$ inch are equivalent to $D=0.4$, $A_2=0.05$. According to Fig. 4, this implies for $\kappa=\pm\frac{1}{2}$, that $\Delta\Gamma=0.47$ or a differential phase shift of 16.9 degrees/cm. The length of the ferrite slabs necessary to obtain a phase shift of 360 degrees is, in general, given by

$$l=\lambda_0/\Delta\Gamma. \tag{7}$$

For our numerical example, this length is 21.3 cm.

It is instructive to consider the dependence of the differential phase shift $\Delta\Gamma$ upon κ, the off-diagonal element of the permeability tensor. For $\kappa\ll 1$, the differential phase shift should obviously be proportional to κ. In Fig. 9, $\Delta\Gamma$ has been plotted vs. κ for $\epsilon=16$, $D=0.4$, and $A_2=0$, 0.05, 0.1, and 0.2. This figure shows that $\Delta\Gamma$ is in fact proportional to κ up to $\kappa=\frac{1}{2}$, to a surprising degree of accuracy. This suggests that the calculation used for determining the curves in Figs. 4–9 could be somewhat simplified by using a perturbation theoretical approach in which κ is treated as small.

III. Losses

The complex circular susceptibilities χ_+ and χ_-, as calculated on the basis of the Landau-Lifshitz equation, can be expressed in the form

$$\chi_+=\frac{M}{H-\dfrac{\omega}{\gamma+i\lambda}}$$
$$\chi_-=\frac{M}{H+\dfrac{\omega}{\gamma-i\lambda}} \tag{8}$$

where M is the saturation magnetization, H the internal magnetic field, ω the angular frequency, γ the gyromagnetic ratio, and the loss parameter λ is (for $\lambda\ll\gamma$) related to the linewidth ΔH by

$$\Delta H\simeq 2\frac{\omega\lambda}{\gamma^2}. \tag{9}$$

In order to apply the result (8) based on the Landau-Lifshitz equation to the behavior at remanence, account must be taken of the fact that the material is not, in general, magnetized to saturation. It has been shown by Rado [6] that this fact can largely be taken into account by replacing the saturation magnetization by the remanent magnetization.

According to (8), the imaginary parts of χ_+ and χ_- become equal for $H=0$ (i.e., at remanence). Thus, $\kappa=2\pi(\chi_+-\chi_-)$ will be real. It appears quite likely that this result is a specific prediction of the Landau-Lifshiftz

equation, which, may not, in general, be absolutely correct. Nevertheless, it is reasonable to assume for a first orientation that κ, is, in fact, real and to calculate the losses to be expected on that basis. In order to simplify the problem, the dielectric losses have also been neglected.

The dielectric and the magnetic contributions to the insertion loss are roughly comparable when the magnetic and dielectric loss tangents are equal. In "good" microwave ferrites, the dielectric loss tangent is of the order of 10^{-4}. The magnetic loss tangent, on the other hand, is usually larger than 10^{-3}. Under these conditions, the dielectric losses can be neglected by way of approximation.

The losses have been calculated only for the case of center loading in the strong field concentration approximation. The relevant characteristic equation is (6) with $A_2=0$. We replace Γ by $\Gamma'-j\Gamma''$, μ by $1-j\mu''$, and μ_e by $\mu'_e-j\mu_e''$ where

$$\mu_e'' = \mu''(1+\kappa^2) \tag{10}$$

since κ is real.

For small Γ'', μ'', and μ_e'' their interrelationship through the imaginary part of the characteristic equation is of the form

$$\Gamma'\Gamma''(\alpha+\beta) = \tfrac{1}{2}\epsilon\mu_e''\alpha + \mu''\gamma \tag{11}$$

where

$$\alpha = [1+\cot^2 D(\epsilon\mu_e - \Gamma'^2)^{1/2}]D - \frac{\kappa\Gamma + \dfrac{\epsilon-\Gamma'^2}{(\Gamma'^2-1)^{1/2}}}{\epsilon\mu_e - \Gamma'^2}$$

$$\beta = -\frac{\kappa}{\Gamma'} + \frac{2}{(\Gamma'^2-1)^{1/2}} + \frac{\epsilon-\Gamma'^2}{(\Gamma'^2-1)^{3/2}}$$

$$\gamma = -\kappa\Gamma' + \frac{\Gamma'^2}{(\Gamma'^2-1)^{1/2}}. \tag{12}$$

As long as dielectric losses can be neglected, Γ'' is proportional to μ''. It is, therefore, convenient to consider the ratio Γ''/μ''. In Fig. 10, this quantity is plotted vs. D for $\epsilon=11$, $\kappa=0$, $\pm\frac{1}{2}$; and, similarly, in Fig. 11 for $\epsilon=16$, $\kappa=\pm\frac{1}{2}$, $\pm\frac{1}{4}$. The expected loss L (in dB) of a phase shift section of length l can be obtained from these graphs by using the relation

$$L = 8.686\cdot 2\pi\frac{l}{\lambda_0}\Gamma''. \tag{13}$$

It should be noticed that Γ''/μ'' depends very little upon κ, at least for $|\kappa|<\frac{1}{2}$ and $D<0.4$. This is especially true for the larger value of ϵ used in the calculation (Fig. 11). This again suggests that a perturbation-theoretical treatment of the characteristic equation, in which κ is treated as small, is adequate for most purposes.

A very important quantity characterizing the performance of phase shifters is the ratio of loss to differential phase shift, or equivalently, the loss of a waveguide

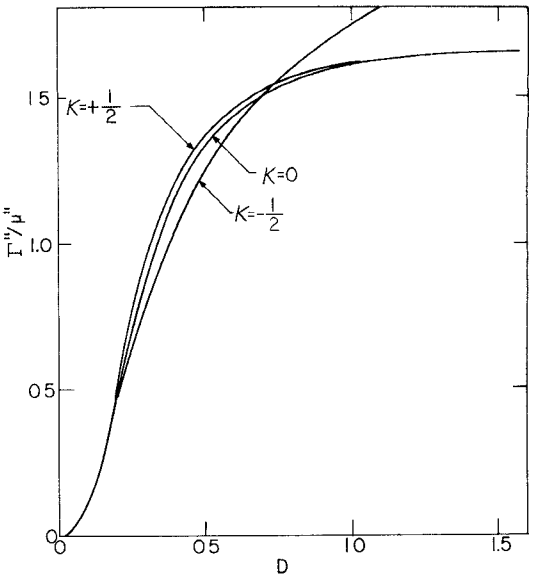

Fig. 10. Imaginary part Γ'' of the reduced propagation constant divided by μ'' plotted vs. reduced slab width D for $A_1=\infty$ (strong field concentration approximation) and $A_2=0$ (center loading). Material constants: $\mu'=1$, $\kappa'=\pm\frac{1}{2}$, $\epsilon'=11$, $\kappa''=0$.

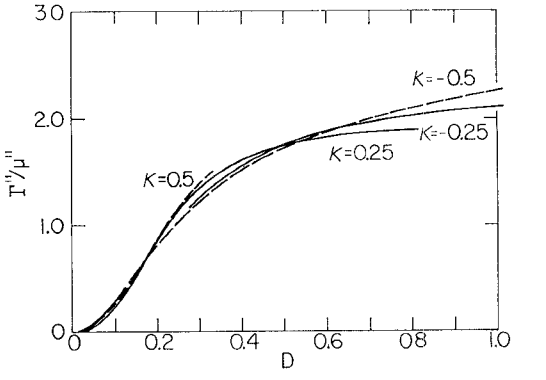

Fig. 11. Imaginary part Γ'' of the reduced propagation constant divided by μ'' plotted vs. reduced slab width D for $A_1=\infty$ (strong field concentration approximation) and $A_2=0$ (center loading). Material constants: $\mu'=1$, $\kappa'=\pm0.25$, ±0.5, $\epsilon'=16$, $\kappa''=0$.

section having a prescribed differential phase shift of, for instance, 2π. This loss, denoted by $L_{2\pi}$, according to (7) and (13) is related to Γ'' and $\Delta\Gamma$ by

$$L_{2\pi} = 8.686\times 2\pi\Gamma''/\Delta\Gamma. \tag{14}$$

Figure 12 shows a plot of $L_{2\pi}$ vs. D for $\epsilon=11$, $\kappa=\pm\frac{1}{2}$, and assuming center loading ($A_2=0$). For the sake of definiteness, it has been assumed that $\mu_e''=0.01$, i.e., $\mu''=0.008$. These numerical values are reasonable for a good ferrite. If the actual value of μ_e'' differs from 0.01, the relevant curve can be obtained by appropriately scaling the vertical axis. The curve of $L_{2\pi}$ vs. D has a rather sharp minimum at $D=0.25$. This corresponds to a slab thickness of approximately $\frac{1}{2.5}$ times the free space wavelength λ_0.

In Fig. 13, similar results for $\epsilon=16$ and $\kappa=\pm\frac{1}{2}$ are shown. The curve for $L_{2\pi}$ is based upon the assumption that $\mu''=0.01$ (rather than 0.008, as in Fig. 12). It should be noticed that the minimum of $L_{2\pi}$ now occurs at a

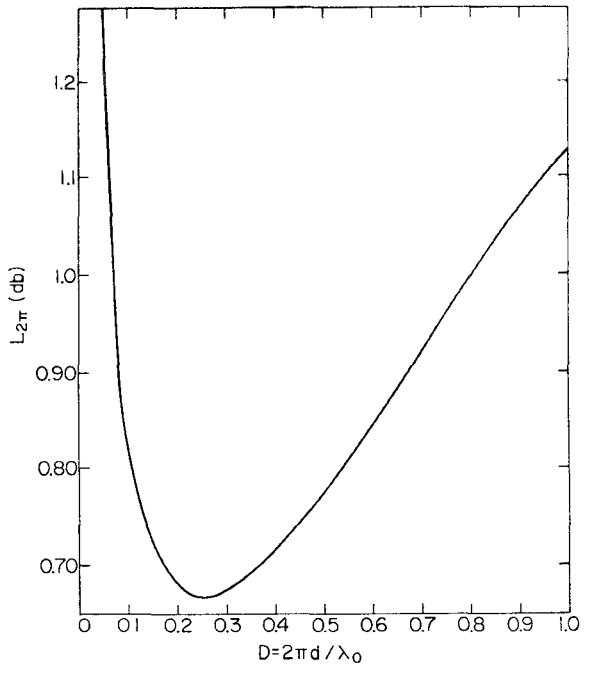

Fig. 12. Calculated insertion loss $L_{2\pi}$ (in dB) of a 360-degree phase shifter vs. reduced slab width D. Assumptions: $A_1=\infty$, $A_2=0$. Material constants: $\mu'=1$, $\kappa'=\pm\frac{1}{2}$, $\mu_e'=\frac{3}{4}$, $\epsilon'=11$, $\mu''=0.008$, $\kappa''=0$, $\mu_e''=0.01$, $\epsilon''=0$.

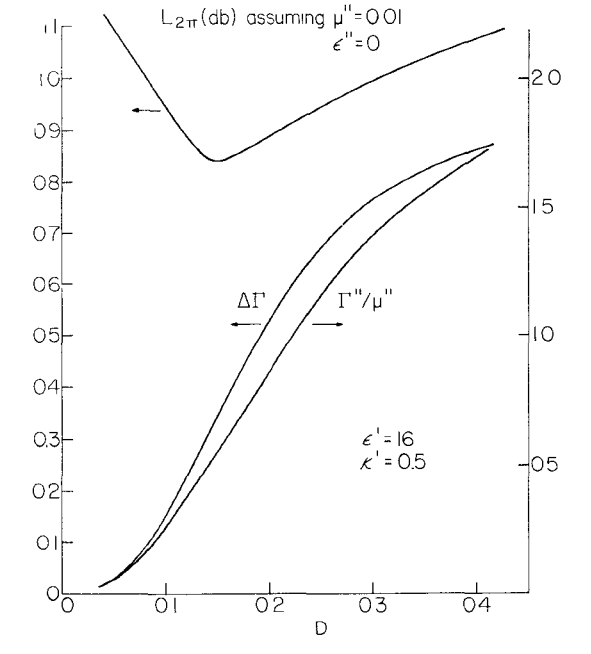

Fig. 13. Reduced differential phase shift $\Delta\Gamma$, imaginary part of the reduced propagation constant Γ'' divided by μ'', and insertion loss $L_{2\pi}$ (in dB) vs. reduced slab width D. Material constants $\mu'=1$, $\kappa'=\pm 0.5$, $\epsilon'=16$.

smaller value of D. The minimum value of $L_{2\pi}$ for a given μ'' is very nearly the same in the two cases considered ($\epsilon=11$ and $\epsilon=16$).

We conclude this section by re-emphasizing the three important assumptions made in this part of the calculation. The assumptions used in addition to the strong field concentration approximation are:

1) neglect of dielectric losses
2) neglect of losses due to κ''
3) center loading.

In comparing experimental data to the theory, these three assumptions should be kept in mind.

IV. Power Handling Capability

It is well known that ferrite phase shifters become lossy at high peak power levels. The critical power level at which this additional loss occurs is determined by the onset of spin-wave instability [7]. The instability sets in when the precession angle (the angle between the instantaneous magnetization and the dc field) exceeds a certain critical value. The threshold condition can also be expressed in terms of the RF magnetic field strength. In order to calculate the power handling capability of the phase shifters under discussion, it is, therefore, first necessary to determine the relationship between the power flowing through the guide and the RF field strength in the ferrite slabs.

The solution of Maxwell's equations for the case of adjacent, oppositely magnetized slabs has been constructed by suitable superposition of plane wave solutions inside the ferrite and by matching these solutions to the exponential solutions outside the ferrite slabs. We assume again that the ferrite slabs are sufficiently thick so that the strong field concentration approximation is applicable. In a coordinate system such as shown in Fig. 14, the RF fields for the symmetric modes are for $0<x<d$

$$h_x = h_{x0}e^{-j\beta y},\quad h_y = jh_{y0}e^{-j\beta y},\quad b_x = b_{x0}e^{-j\beta y} \tag{15}$$

where

$$\begin{aligned} h_{x0} &= h_0\left[\cos k_m x - \frac{\kappa\epsilon}{\Gamma(\mu_e\epsilon-\Gamma^2)^{1/2}}\sin k_m x\right] \\ h_{y0} &= h_0\frac{\mu\epsilon-\Gamma^2}{\Gamma(\mu_e\epsilon-\Gamma^2)^{1/2}}\sin k_m x \\ b_{x0} &= \mu h_{x0}+\kappa h_{y0} \\ &= h_0\left[\mu\cos k_m x - \frac{\kappa\Gamma}{(\mu_e\epsilon-\Gamma^2)^{1/2}}\sin k_m x\right] \\ e_z &= b_x/\Gamma \end{aligned} \tag{16}$$

and for $x>d$

$$\begin{aligned} h_x &= Ah_0e^{-\alpha(x-d)}e^{-j\beta y} \\ h_y &= j\frac{(\Gamma^2-1)^{1/2}}{\Gamma}h_x \\ e_z &= h_x/\Gamma \end{aligned} \tag{17}$$

where

$$\begin{aligned} A &= \frac{(\mu\epsilon-\Gamma^2)\sin k_m d}{(\Gamma^2-1)^{1/2}(\mu_e\epsilon-\Gamma^2)^{1/2}} \\ k_m &= (\omega/c)(\epsilon\mu_e-\Gamma^2)^{1/2} \\ \alpha &= [\beta^2-(\omega/c)^2]^{1/2} = \omega/c(\Gamma^2-1)^{1/2}. \end{aligned} \tag{18}$$

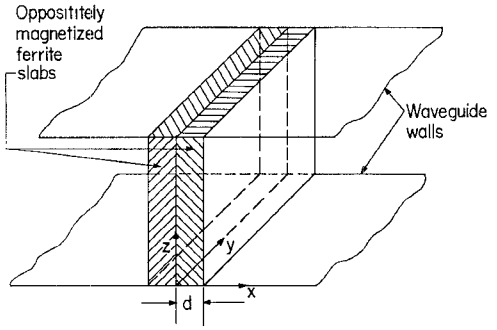

Fig. 14. Coordinate system used in Section IV.

For $x<0$, the solution (15)–(18) must be continued in such a way that h_x, b_x, and e_z are symmetric, and h_y and b_y are antisymmetric. h_0 is obviously the strength of the transverse RF magnetic field in the center of the waveguide (i.e., at $x=0$).

It can readily be verified that the solution (15)–(18) indeed satisfies Maxwell's equations as well as all boundary conditions. It is apparent that e_z, h_y, and b_x are continuous at $x=0$ (the interface between the two oppositely magnetized ferrite slabs). Furthermore, h_y is obviously continuous at $x=d$. The condition that b_x and e_z be continuous at $x=d$ leads to the characteristic equation

$$\cot k_m d = \frac{1}{\mu(\mu_e\epsilon - \Gamma^2)^{1/2}}\left[\kappa\Gamma + \frac{\epsilon\mu - \Gamma^2}{(\Gamma^2-1)^{1/2}}\right] \tag{19}$$

which is a special case ($A_2=0$) of the more general characteristic equation (6).

The time average of the energy flow per unit area in the y direction is

$$S = \frac{1}{2}\frac{c}{4\pi} e_z h_x^* \tag{20}$$

where the asterisk denotes the complex conjugate. Thus, from (15) and (16) for $0<x<d$

$$S = \frac{ch_0^2}{16\pi\Gamma^2(\mu_e\epsilon - \Gamma^2)}\{\Gamma\mu(\mu\epsilon - \Gamma^2) + \Gamma[(\mu^2 - 2\kappa^2)\epsilon - \mu\Gamma^2]\cos 2k_m x - \kappa(\mu_e\epsilon - \Gamma^2)^{1/2}(\Gamma^2 + \epsilon\mu)\sin 2k_m x\} \tag{21}$$

whereas, for $x>d$ from (17) and (18),

$$S = \frac{ch_0^2(\mu\epsilon - \Gamma^2)^2 \sin^2 k_m d}{8\pi(\Gamma^2-1)(\mu_e\epsilon - \Gamma^2)\Gamma} e^{-2\alpha(x-d)}. \tag{22}$$

The relationship between the power flowing through the guide and the RF magnetic field strength depends, of course, upon the height of the waveguide. We assume, for simplicity, that the height of the guide equals one quarter of the free space wavelength. The power traveling through the interior of the ferrite slabs is, thus, according to (21),

$$P_{\text{in}} = \frac{\pi c}{\omega}\int_0^d S\,dx = \frac{c^3 h_0^2}{16\omega^2} p_{\text{in}} \tag{23}$$

where

$$p_{\text{in}} = \frac{1}{\Gamma^2(\mu_e\epsilon - \Gamma^2)}\{\Gamma\mu(\mu\epsilon - \Gamma^2)D + \frac{\Gamma[(\mu^2 - 2\kappa)\epsilon - \mu\Gamma^2]}{(\mu_e\epsilon - \Gamma^2)^{1/2}}\sin k_m d\cos k_m d - \kappa(\Gamma^2 + \mu\epsilon)\sin^2 k_m d\}. \tag{24}$$

Similarly, the power traveling through the exterior of the ferrite slabs is, according to (22),

$$P_{\text{out}} = \frac{\pi c}{\omega}\int_d^\infty S\,dx = \frac{c^3 h_0^2}{16\omega^2} p_{\text{out}} \tag{25}$$

where

$$p_{\text{out}} = \frac{(\mu\epsilon - \Gamma^2)^2 \sin^2 k_m d}{(\Gamma^2-1)^{3/2}(\mu_e\epsilon - \Gamma^2)\Gamma}. \tag{26}$$

By using the characteristic equation (19), the reduced powers p_{in} and p_{out} can also be expressed as

$$p_{\text{in}} = \frac{\mu}{\Gamma^2(\mu_e\epsilon - \Gamma^2)}\left\{\Gamma(\mu\epsilon - \Gamma^2)D + \frac{\Gamma(\Gamma^2-1)^{1/2}[(\mu^2 - 2\kappa^2)\epsilon - \mu\Gamma^2] - \mu\mu_e\kappa\epsilon(\Gamma^2-1)}{\mu\epsilon - \Gamma^2 + \mu\mu_e(\Gamma^2-1) + 2\kappa\Gamma(\Gamma^2-1)^{1/2}}\right\} \tag{27}$$

$$p_{\text{out}} = \frac{(\mu\epsilon - \Gamma^2)\mu^2}{\Gamma(\Gamma^2-1)^{1/2}[\mu\epsilon - \Gamma^2 + \mu\mu_e(\Gamma^2-1) + 2\kappa\Gamma(\Gamma^2-1)^{1/2}]}. \tag{28}$$

In Fig. 15(a) and (b), p_{in}, p_{out}, and $p=p_{\text{in}}+p_{\text{out}}$ are plotted vs. the reduced slab thickness for a representative case ($\mu=1$, $\kappa=\pm\frac{1}{2}$, $\epsilon=11$).

It should be noticed that in the vicinity of $D=0.25$ (i.e., the thickness, at which the insertion loss $L_{2\pi}$ is a minimum) the values of p applicable for $\kappa=+\frac{1}{2}$ and $\kappa=-\frac{1}{2}$ are significantly different ($p=0.21$ for $\kappa=+\frac{1}{2}$ and $p=0.74$ for $\kappa=-\frac{1}{2}$). This implies that the power handling capability in the two states of the phase shifter is significantly different. Since the lower value of p determines the useful power range of the device, we obtain from (23), (25), and (27)

$$P = 3.31\times 10^{-4} c\lambda_0^2 h_0^2. \tag{29}$$

A useful rule of thumb which is equivalent with (29) is as follows: If $\lambda_0=10$ cm and $h_0=10$ Oe, then $P\simeq 10$ kW.

Consider now the instability threshold. The strength of the RF field, in general, is different in different parts of the sample. It is not immediately obvious at which point within the sample instability will first set in. It is shown in the Appendix that, to a reasonably good approximation, the threshold is entirely determined by the

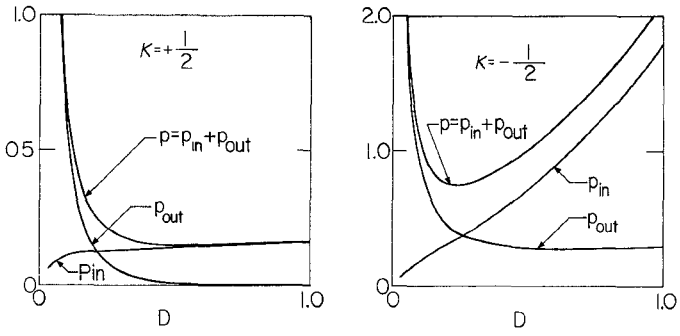

Fig. 15. Power (in reduced units) flowing through the interior (p_{in}) and exterior (p_{out}) of the ferrite slabs at a fixed value of RF magnetic field amplitude plotted vs. reduced slab thickness. Assumptions: $A_1=\infty$, $A_2=0$, $\mu'=1$, $\epsilon'=11$, $\kappa'=+\frac{1}{2}$ (a), $\kappa'=-\frac{1}{2}$ (b).

positive circular component of the uniform precession. Here, the positive sense of circular polarization is defined as that sense of polarization whose direction agrees with the direction of the free precession of the magnetization vector; or, equivalently, as that sense of polarization which, together with the direction of dc magnetization, forms a right-handed screw.

At remanence, the diagonal component of the permeability tensor is unity to a good approximation. Thus, the directional cosines of the magnetization vector with respect to the x and y axes are for $0<x<d$

$$\alpha_x = -j\kappa h_y/4\pi M = (\kappa h_{y0}/4\pi M)e^{j(\omega t-\beta y)}$$
$$\alpha_y = j\kappa h_x/4\pi M = (j\kappa h_{x0}/4\pi M)e^{j(\omega t-\beta y)}, \tag{30}$$

where h_{x0} and h_{y0} are given by (16). The positive circular component of the uniform precession is

$$|\alpha_+| = \frac{|\kappa|}{8\pi M}|h_{x0}-h_{y0}|. \tag{31}$$

By plotting the quantity $(h_{x0}-h_{y0})$ vs. x for a representative case, it can be shown that the positive circular component of the uniform precession has its largest value at $x=0$. Thus, instability will tend to occur there first.

The power handling capability of ferrite phase shifters can most conveniently be discussed by introducing a high-power "figure of merit" [8] F_{hp} as follows

$$F_{hp} = \frac{4\pi M_r\gamma^2 h_{crit}^{(c.p.)}}{\omega^2\mu''}. \tag{32}$$

Here M_r is the remanent magnetization and $h_{crit}^{(c.p.)}$ is the critical field for spin-wave instability measured at remanence using circular polarization. In previous work [8], we have shown that the high-power figure of merit as defined by (32) is subject to some rather fundamental theoretical limitations and have also presented experimental data. The theoretical discussion, as well as the experimental data, indicate that a high-power figure of merit of approximately one can be achieved in practice. Significantly larger values of F_{hp} can, according to theory, be achieved only by reducing the saturation magnetization [8]. The theory, which leads to this prediction, is based on the assumption that the absorption line has a "Lorentzian" shape. This assumption is well justified in materials containing significant amounts of "strong relaxers" such as Dy^{++}, Ho^{++}, Fe^{++} or Co^{++}, but does not apply to materials which do not contain strong relaxers.

The critical power level P_{crit} of a twin-slab phase shifter can, of course, be expressed rather simply in terms of the critical RF field h_{crit} [see (29)], and it is not necessary to introduce the high-power figure of merit. The advantage of expressing P_{crit} in terms of the high power figure of merit lies in the fact that the relationship between insertion loss and power handling capability is put into evidence. At the same time, the ultimate limitations of phase shifters with a given insertion loss are clearly indicated.

Using the definition (32), and (23), (25) and (27), the critical power level can be expressed in terms of $L_{2\pi}$ and F_{hp} by the relation

$$P_{crit} = P_0 L_{2\pi}^2 F_{hp}^2 \tag{33}$$

where

$$P_0 = \frac{c^3 p}{4\gamma^2}\left(\frac{\Delta\Gamma/\kappa'}{8.686\cdot 2\pi\Gamma''/\mu''}\right). \tag{34}$$

Here we have used the facts that $\kappa'=\gamma 4\pi M_r/\omega$, and that the circular component of the magnetic field at the interface of the two slabs equals $\frac{1}{2}h_0$. It should be noticed that the power P_0 as defined by (34) depends only very weakly on the properties of the material because $\Delta\Gamma$ is proportional to κ' and Γ'' proportional to μ'' to a good approximation. P_0 and, hence, the critical power are, of course, functions of the reduced slab thickness D, because in (34) p, $\Delta\Gamma/\kappa'$, Γ''/μ'' depend upon D. For the previously used numerical example ($\epsilon=11$, $\kappa=\pm\frac{1}{2}$, $D=0.25$, $A_2=0$, $p=0.21$, $\Delta\Gamma/\kappa'=0.9$, $\Gamma''/\mu''=0.75$) one obtains, according to (34),

$$P_0 \simeq 220 \text{ kW}. \tag{35}$$

In the calculation of the critical power level, it was assumed that the separation of the two slabs is vanishingly small. This configuration cannot be realized in practice. It appears likely that for small slab separations the ratio of the power flowing through the guide to the square of the maximum RF magnetic field strength in the ferrite will not be changed significantly. This implies that the power P_0 calculated in accordance with (33) and (34) will change appreciably with slab spacing because $\Delta\Gamma/\kappa'$ depends quite sensitively upon A_2. For instance, taking A_2 as 0.05 (i.e., a slab spacing $2a_2$ of 0.016 λ_0) and taking all the other parameters as in the preceding example, reduces the numerical value of P_0 from 220 kW to 120 kW.

It appears likely that a high-power figure of merit of the order of unity can be achieved in practice. The predicted critical power level of a phase shifter having an

insertion loss of 1 dB is, thus, of the order of 100 kW. This value will be further reduced if account is taken of the dielectric loss. Another important consideration is the fact that the critical RF field usually changes significantly with temperature. This also tends to reduce the attainable peak power capability.

Note

The performance of twin-slab phase shifters has also recently been analyzed by Ince and Stern [9]. These authors have considered the case in which the space between the two slabs is filled with a suitable dielectric. Considerable improvement in differential phase shift can be obtained in this manner.

Appendix
First-Order Spin-Wave Instability Excited by Elliptical Precession of the Uniform Magnetization

The equation of motion for the amplitude

$$\delta\alpha = \delta\alpha_x + i\delta\alpha_y$$

of a standing spin wave can be expressed as

$$\delta\dot{\alpha} = i(a\delta\alpha + b\delta\alpha^*) \tag{36}$$

where

$$\begin{aligned} a &= a_0 + a_{11}\alpha + a_{11}{}^*\alpha^* \\ b &= b_0 + 2a_{11}{}^*\alpha \end{aligned} \tag{37}$$

and

$$\alpha = \alpha_x + i\alpha_y \tag{38}$$

is the amplitude of the uniform mode. The analytic expressions for a_0, b_0, and a_{11} are given in Schlömann et al. [10], equation (38).

If the uniform precession is not excited ($\alpha=0$), the equation of motion for the spin wave can be transformed into the form

$$\delta\beta = i\omega_k\delta\beta \tag{39}$$

by means of the transformation

$$\delta\alpha = \delta\beta + \lambda\delta\beta^*. \tag{40}$$

The parameter λ in this transformation is given in Schlömann et al. [10], equation (52).

If the uniform precession is excited, the right-hand side of (39) is modified by the addition of terms proportional to $\delta\beta$ and $\delta\beta^*$ which are also proportional to α or α^* and, are, hence, time dependent. The time-dependent factor of $\delta\beta$ is irrelevant and will be omitted because it does not influence the instability threshold (at least not to lowest order). The complete equation of motion for $\delta\beta$ can be expressed as

$$\delta\beta = i[\omega_k\delta\beta + f(t)\delta\beta^*] \tag{41}$$

where

$$f(t) = 2(1 - |\lambda|^2)^{-1}(a_{11}{}^* + \lambda a_{11})(\alpha + \lambda\alpha^*). \tag{42}$$

Under typical conditions encountered in practical applications, the transformation parameter λ is small in magnitude, being given (approximately) by

$$|\lambda| \simeq \frac{1}{2}\,|b_0|/a_0 \simeq \frac{1}{4}\,\frac{\omega_M}{\omega_k}\sin^2\theta. \tag{43}$$

Since the important spin waves have $\theta\simeq\pi/4$, we find for $\omega_M/\omega_k = 1$

$$|\lambda| \simeq \tfrac{1}{8}. \tag{44}$$

Under these conditions, it is permissible to neglect the terms containing λ in (42) by way of approximation. The factor $f(t)$ of $\delta\beta^*$ in this equation is, thus,

$$\begin{aligned} f_k &= 2a_{11}{}^*\alpha \\ &= -\omega_M \sin\theta\cos\theta e^{i\phi}\alpha. \end{aligned} \tag{45}$$

If the uniform precession is elliptical, the time dependence of α is given by

$$\alpha = \alpha_+ e^{i\omega t} + \alpha_- e^{-i\omega t}. \tag{46}$$

Only the positive circular component α_+ of the uniform precession gives rise to instability. The instability threshold is

$$|\alpha_+|_{\text{crit}} = \frac{\eta}{\omega_M \sin\theta\cos\theta}$$

where η is the relaxation rate of the spin wave under consideration.

Acknowledgment

The author is greatly indebted to Mrs. C. King and Howard Graichen for their help with the numerical calculations, and to J. J. Green for discussions concerning the experimental aspects of the problem.

References

[1] M. A. Treuhaft and L. M. Silber, "Use of microwave ferrite toroids to eliminate external magnets and reduce switching powers," *Proc. IRE (Correspondence)*, vol. 46, p. 1538, August 1958.
[2] L. Levey and L. M. Silber, "A fast-switching X-band circulator utilizing ferrite toroids," *1960 IRE WESCON Conv. Rec.*, pp. 11–20.
[3] B. Lax, K. J. Button, and L. M. Roth, "Ferrite phase shifters in rectangular waveguide," *J. Appl. Phys.*, vol. 25, pp. 1413–1421, November 1954.
[4] B. Lax and K. J. Button, *Microwave Ferrites and Ferrimagnetics*. New York: McGraw-Hill, 1962, pp. 323–354.
[5] W. H. von Aulock, *Ferrite Devices for Microwave Application*. Englewood Cliffs, N. J.: Prentice-Hall, to be published.
[6] G. T. Rado, "Theory of the microwave permeability tensor and Faraday effect in nonsaturated ferromagnetic materials," *Phys. Rev.*, vol. 89, p. 529, January 1953.
[7] For a recent review on this subject see, for instance, the article by R. W. Damon in *Magnetism*, vol. 1, G. T. Rado and H. Suhl, Eds., New York: Academic, 1963.
[8] E. Schlömann, J. J. Green, and J. H. Saunders, "Ultimate performance limitations of high-power ferrite circulators and phase shifters," *IEEE Trans. on Magnetics*, vol. MAG-1, pp. 168–174, September 1965.
[9] W. J. Ince and E. Stern, "Waveguide non-reciprocal remanence phase shifters," presented at the 1965 Internat'l Conf. on the Microwave Behavior of Ferrimagnetics and Plasmas, London, A brief description of this work was given at the 1965 G-MTT meeting in Clearwater, Fla.
[10] E. Schlömann, R. I. Joseph, and I. Bady, "Spin-wave instability in hexagonal ferrites," *J. Appl. Phys.* vol. 34, pp. 672–681, March 1963.